Direct photochemistry of three fluoroquinolone antibacterials: Norfloxacin, ofloxacin, and enrofloxacin

6 AUTHORS, INCLUDING:

Kristine H Wammer
University of St. Thomas
10 PUBLICATIONS **255** CITATIONS

SEE PROFILE

Rachel Lundeen
University of Washington Seattle
7 PUBLICATIONS **61** CITATIONS

SEE PROFILE

Kristopher McNeill
ETH Zurich
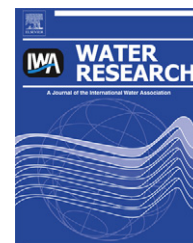**126** PUBLICATIONS **3,415** CITATIONS

SEE PROFILE

William A Arnold
University of Minnesota Twin Cities
118 PUBLICATIONS **3,898** CITATIONS

SEE PROFILE

ELSEVIER

WATER RESEARCH
A Journal of the International Water Association

Direct photochemistry of three fluoroquinolone antibacterials: Norfloxacin, ofloxacin, and enrofloxacin

Kristine H. Wammer [a,*], *Andrew R. Korte* [a], *Rachel A. Lundeen* [a], *Jacob E. Sundberg* [a], *Kristopher McNeill* [b], *William A. Arnold* [c]

[a] *Department of Chemistry, University of St. Thomas, 2115 Summit Ave., St. Paul, MN 55105, USA*
[b] *Institute for Biogeochemistry and Pollutant Dynamics, ETH Zurich, 8092 Zurich, Switzerland*
[c] *Department of Civil Engineering, University of Minnesota, 500 Pillsbury Dr. SE, Minneapolis, MN 55455, USA*

ARTICLE INFO

ABSTRACT

Fluoroquinolone (FQ) antibacterial compounds are frequently detected in the aquatic environment, and photodegradation is expected to play an important role in FQ fate in some sunlit surface waters. This study investigated the direct aquatic photochemistry of three FQs: norfloxacin, ofloxacin, and enrofloxacin. The direct photolysis rate of each drug exhibited strong pH dependence when exposed to simulated sunlight. For each FQ, direct photolysis rates and total light absorbance were used to calculate quantum yields for each of three environmentally relevant protonation states: a cationic, a zwitterionic, and an anionic form. In each case, quantum yields of the species varied significantly. The quantum yield for the zwitterionic form was 2–3 times higher than that of the anionic form and over an order of magnitude higher than that of the cationic form. Antibacterial activity assays were used to determine whether the loss of parent FQ due to photolysis led to loss of activity. Norfloxacin and ofloxacin photoproducts were found to be inactive, whereas enrofloxacin photoproducts were found to retain significant activity. These results are important for aiding in predictions of the potential impacts of FQs in surface waters.

1. Introduction

Fluoroquinolones (FQs) are a class of antibacterial compounds used extensively in both human and veterinary medicine. FQs have been found in hospital wastewaters (at concentrations ranging from approximately 60–120,000 ng/L), in wastewater treatment plant (WWTP) effluents (∼2–580 ng/L) and in surface waters (∼5–1300 ng/L) throughout the world, including in the United States (Kolpin et al., 2002; Renew and Huang, 2004), Italy (Andreozzi et al., 2003), Switzerland (Giger et al., 2003; Golet et al., 2003), Finland (Vieno et al., 2007), Sweden (Lindberg et al., 2006), Germany (Hartmann et al., 1999), China (Xu et al., 2009), and Australia (Watkinson et al., 2009).

Research about which processes are most likely to control the environmental fate of FQs in aquatic environments is needed to assess potential long-term impacts. The presence of FQs and other antibacterial compounds in the environment is of concern primarily due to the possibility that long-term exposure to sub-therapeutic doses may provide selective pressure for antibiotic-resistant organisms (Kümmerer, 2009). There is also concern that FQs may inhibit photosynthesis in plants (Aristilde et al., 2010). Previous work has shown that photodegradation is expected to play an important role in FQ fate in some sunlit surface waters (Schmitt-Kopplin et al., 1999; Andreozzi et al., 2003; Knapp et al., 2005; Lam and Mabury, 2005; Sturini et al., 2010; Li et al., 2011), and in particular may be significant relative to other abiotic

processes, such as sorption, in waters with low particulate organic carbon (POC) (Cardoza et al., 2005). A recent study focused on the photochemical fate of eight FQs in different natural waters (Ge et al., 2010). In the study, photolysis rates of the two drugs studied in detail (sarafloxacin and gatifloxacin) exhibited a strong pH dependence, which must be due to variations in absorption spectra and/or quantum yields for species with different protonation states. Quantifying these variations would aid in the prediction of FQ degradation rates in a range of natural waters.

In this work, the direct photochemical behavior of three FQs was investigated: norfloxacin (NOR), ofloxacin (OFL), and enrofloxacin (ENR). NOR and OFL are used primarily in human medicine and ENR is used in veterinary medicine. All of these FQs have been detected in WWTP effluents and/or natural waters (e.g. Kolpin et al., 2002; Andreozzi et al., 2003; Giger et al., 2003; Renew and Huang, 2004; Watkinson et al., 2009). Direct photolysis degradation rates and total light absorbance were used to calculate quantum yields for each of three environmentally relevant protonation states for each drug. This analysis is necessary for accurate prediction of photolysis rates over the range of pH values (typically between 6 and 9) found in natural waters. In addition, bacterial assays were used to determine whether loss of parent FQ due to direct photolysis correlates with loss of antibacterial activity because any FQ intermediates or photoproducts retaining the ability to inhibit bacterial growth could potentially have long-term effects on antibiotic resistance. Selected photoproducts were isolated, characterized, and assessed for activity.

2. Material and methods

2.1. Reagents and materials

ENR (98%), NOR (98%), and ciprofloxacin (CIP, 98%) were purchased from Sigma—Aldrich. OFL (99+%) was purchased from MP Biomedicals Inc. Pyridine (99+%), p-nitroanisole (PNA; 99+%), and Iso-Sensitest bacterial growth medium were supplied by Thermo Fisher Scientific. Tryptone and yeast extract were purchased from Becton, Dickinson and Company. All chemicals were used as received. Solvents were of HPLC grade. Deionized water was purified using a Barnstead Nanopure system.

2.2. Natural water photolysis

Stock solutions of each FQ in deionized water (100 μM) were diluted to 10 μM using deionized water or filtered Lake Josephine water (St. Paul, MN, DOC ~6 mg/L, filtered through 0.2 μm filters). Lake Josephine water solutions of each drug were photolyzed alongside deionized water solutions. The deionized water samples were adjusted to a pH similar to that of the natural water samples (7.8—7.9) using small amounts (approximately 1—10 μL) of NaOH or HCl. Solutions for photolysis were placed in 13 mm × 100 mm quartz test tubes in a rack at an angle of approximately 30° to the horizontal. Photolyses were conducted in an Atlas Suntest CPS + solar simulator equipped with a xenon lamp and an Atlas UV Suntest filter, to provide an emission spectrum accurately

simulating that of natural sunlight and an irradiance of 765 W/m^2 (see Fig. S1). At pre-determined time intervals, aliquots were removed from the tubes and stored in the dark until analysis. The pH of each sample was measured before and after each photolysis experiment to ensure no significant changes over the course of the experiment.

2.3. HPLC analyses

High performance liquid chromatography (HPLC) analysis was conducted using an Agilent 1100 Series chromatograph with an ultraviolet—visible (UV—Vis) diode array detector. All samples were adjusted to similar pH by addition of a small amount of strong base (6 M NaOH) prior to analysis. The column used was a Supelco Discovery RP Amide C_{16} (100 mm × 4.6 mm, 5 μm particle size). The mobile phase was an isocratic 85:15 mixture of pH 3 phosphate buffer (8.7 mM): acetonitrile at a 1.0 ml per minute flow rate. NOR and ENR were detected at 271 nm while OFL was detected at 286 nm.

2.4. pK$_a$ and quantum yield determination

The pH of 50 μM solutions of individual FQs in deionized water was adjusted to a range of values (approximately 3—11) by addition of small amounts (approximately 1—10 μL) of NaOH or HCl. UV—Vis absorbance spectra were obtained of each solution on a Hewlett Packard 8452A spectrophotometer to use for determination of pK$_a$ values. Similar pH-adjusted solutions of each FQ (10 μM) were used for quantum yield determination. Approximately 2 mL of each solution was removed and used to obtain UV—Vis spectra, which were then deconvoluted according to the method of Boreen et al. (2004) to obtain molar absorptivities for the three relevant protonation species of each drug. The remaining sample was then irradiated in the solar simulator and aliquots were removed at pre-determined time intervals and analyzed by HPLC as described above. Photolyses were conducted alongside a PNA/pyridine actinometer solution prepared according to Leifer with a quantum yield of 0.00465 (Leifer, 1988).

2.5. Antibacterial activity screening

The ability of each FQ to inhibit growth of Escherichia coli DH5α was determined as described previously (Wammer et al., 2006). E. coli were grown overnight on Iso-Sensitest broth (ISB, made by adding 23.4 g of ISB powder per liter of pH 7 phosphate buffer (4.9 g KH_2PO_4 and 9.7 g Na_2HPO_4 in deionized water)) and sterilized by autoclaving (20 min; 121 °C; 15 psig). Aliquots of E. coli (100 μL) and the appropriate volume of unirradiated 100 μM FQ solution were added to test tubes containing 9 mL of sterile ISB to obtain a range of FQ concentrations varying from approximately 0.01—10 μM. Test tubes were incubated in the dark for six (ENR) or eight (NOR, OFL) hours (37 °C, 200 rpm). Bacterial growth was assessed by measuring optical density at 600 nm and comparing to initial optical density of each solution (final OD_{600}—initial OD_{600}).

To assess the ability of FQ photoproduct mixtures to inhibit E. coli growth, FQ solutions (100 μM) were photolyzed as described above and samples were collected over time. Photolysate (photoproduct mixture plus remaining parent

fluoroquinolone, 1 ml) from each time point was added to the test tubes in place of the 1 ml of unirradiated FQ. The photolysate samples corresponding to each time point were analyzed by HPLC to determine the amount of parent FQ remaining. The antibacterial activity of selected isolated photoproducts or groups of photoproducts (isolated by preparative HPLC, see below) was assessed in a similar manner with the exception that, without an authentic standard for unknown photoproducts, concentration of the photoproducts could not be quantified by HPLC. Only a qualitative assessment of whether activity was observed could be made. All bioassays were performed in triplicate.

2.6. Selected Photoproduct characterization

Solutions of ENR (500 μM) in deionized water were irradiated outdoors (under summer sunlight in St. Paul, MN, 45° N latitude) or in the solar simulator for a long enough period of time (approximately one half life) to generate significant quantities of major photoproducts. Because this set of experiments was not used to generate data about photolysis rates, it was not of concern that these solutions were not optically dilute. Following photolysis, the resultant mixtures of products and residual parent compound were concentrated via rotary evaporation. Selected photoproducts (see Section 3.5 for details) were isolated by preparative HPLC, using a Supelco Discovery RP Amide C_{16} column (100 mm × 21.2 mm, 5 μm particle size), a 5 mL per minute flow rate, an isocratic 85:15 mixture of pH 3 formic acid buffer : acetonitrile, and the same detection as described above. Fractions were collected, concentrated again, and stored in the dark to prevent degradation of photolabile products. High-resolution mass spectra of each isolated product were obtained on a Bruker BioTOF II instrument equipped with an ESI source using polyethylene glycol (PEG) as an internal reference standard. Spectra were obtained under positive ionization mode. A JEOL 400 MHz nuclear magnetic resonance (NMR) spectrometer was used to obtain a fluorine NMR spectrum of one isolated ENR product.

3. Results and discussion

3.1. Natural water photolysis

Previous work has shown that direct photolysis, rather than indirect photolysis involving interactions with natural water constituents, is likely to be the dominant photolysis process for FQs in most natural waters (Schmitt-Kopplin et al., 1999; Cardoza et al., 2005; Lam and Mabury, 2005; Prabhakaran et al., 2009; Li et al., 2011) with the exception of one study in which enhanced OFL degradation was observed in the presence of humic acids and nitrate (Andreozzi et al., 2003). Most comprehensively, Ge et al. (2010) used a central composite design to determine individual effects of various freshwater and seawater constituents and found that several (i.e., humic acids, Fe^{3+}, and NO_3^-) inhibited rather than enhanced FQ photolysis rates. Li et al. (2011) observed self-sensitized photolysis for ENR, but this was at significantly higher concentrations (10 mg/L) than would be expected in environmentally relevant samples;

self-sensitization is unlikely at the concentrations typically observed in natural waters.

In the present study, the three FQs of interest were irradiated in a local natural water sample (Lake Josephine) simultaneously alongside deionized water samples adjusted to the same pH (all at pH 7.8—7.9). Photolysis was rapid for all three drugs ($t_{1/2}$ = 1—4 min) and followed apparent first-order kinetics (Fig. 1). Any significant indirect photochemical pathways (e.g. reaction with excited state dissolved organic matter (DOM) or with photochemically produced reactive intermediates such as singlet oxygen ($^1O_2$)) would have been seen as enhanced photodegradation in the Lake Josephine water. This was not observed. The slightly slower degradation rate in the natural water samples may be attributable to light screening by DOM, or the DOM may be preventing oxidation by quenching an excited triplet state (Ge et al., 2010; Li et al., 2011; Wenk et al., 2011). Because direct photolysis will clearly be an important process, if not the primary photodegradation pathway in most natural waters, all subsequent experiments focused on direct photolysis and were conducted in deionized water.

3.2. pK_a determination

Table 1 shows the dominant protonation state of each of the three FQs at neutral pH, which is a zwitterionic form. There are two relevant acid—base processes for FQs within the range of pH values encountered in natural waters. The first (pK_{a1}) involves the proton on the carboxylic acid group while the second (pK_{a2}) applies to the external amino group on the piperazine ring (Lizondo et al., 1997; Ross and Riley, 1992). At more acidic pH values, the most prevalent form of these molecules will be cationic and at more basic pH values an anionic form will be dominant. Apparent macroscopic dissociation constants corresponding to pK_{a1} and pK_{a2} in the literature are somewhat variable. For example, reported pK_{a1} values for ENR range from approximately 5.8 to 6.3 (Golet et al., 2003; Schmitt-Kopplin et al., 1999; Lizondo et al., 1997; Jiménez-Lozano et al., 2002; Qiang and Adams, 2004). The pK_a values, therefore, were measured directly by spectrophotometric titration rather than attempting to select appropriate values from the literature.

The absorbance spectra are shown in the SI (Figs. S2—S4). The absorbance at a single wavelength (282 nm for NOR, 292 nm for OFL, and 336 nm for ENR) was plotted against pH and pKa values were determined by fitting the data to Equation (1):

$$\left(\chi_{FH_2^+}\right)\left(A_{FH_2^+\lambda}\right) + \left(\chi_{FH}\right)\left(A_{FH\lambda}\right) + \left(\chi_{F^-}\right)\left(A_{F^-\lambda}\right) \equiv A_{tot} \quad (1)$$

where χ refers to the fraction of the cationic (FH_2^+), zwitterionic (FH), and anionic (F^-) species present, and A is absorbance at a selected wavelength. This fit is also shown in Figs. S2—S4. Due to lack of a good fit, the pK_{a2} value for ENR was obtained from the literature; the selected value was obtained via capillary electrophoresis with diode array detection (CE-DAD) using absorbance spectra obtained at the maximum of electrophoretic peaks at a range of pH values (Jiménez-Lozano et al., 2002).

The pK_{a1} values for each compound are close to each other in value, and are higher than in comparable compounds (e.g. benzoic acid pK_a = 4.20) due to the ability of the carboxylic acid proton to form an intramolecular hydrogen bond with the
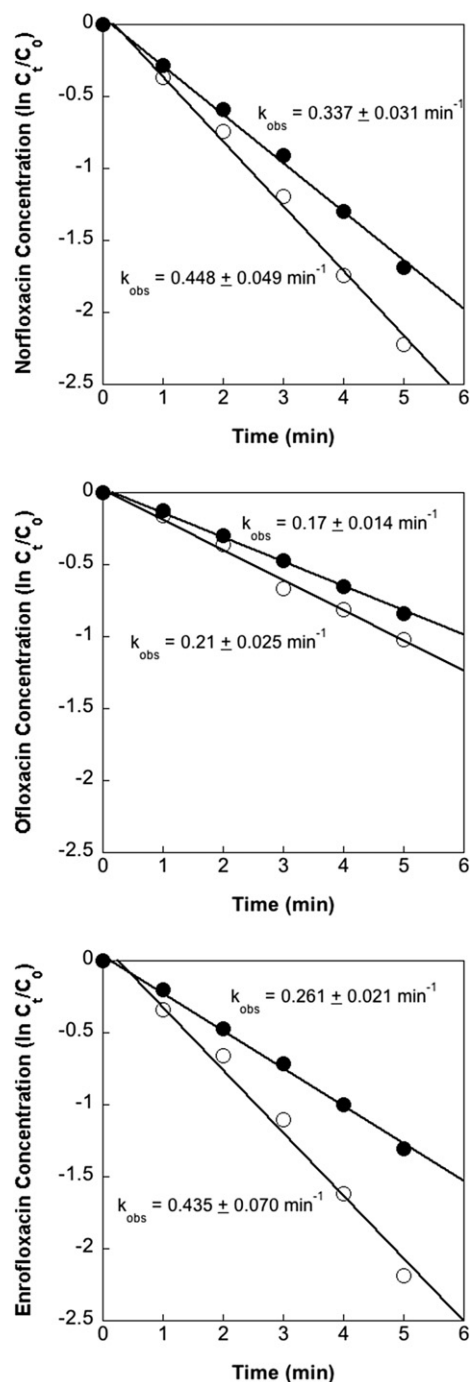
Table 1 – Structures and experimentally determined pK_a values for three FQs: NOR, OFL, and ENR. FQ ring numbering convention is illustrated on the NOR structure.

Compound	Structure	pK_a values
Norfloxacin		6.11 9.11
Ofloxacin		6.05 8.72
Enrofloxacin		6.2 7.9[a]

a   Jiménez-Lozano et al., 2002

Fig. 1 – Loss of three fluoroquinolones (norfloxacin, ofloxacin, and enrofloxacin) over time during photolysis in deionized water (open circles) and Lake Josephine water (closed circles). Rate constants (k_{obs}) were determined via linear regression and the errors are the 95% confidence intervals of the regressed value.

keto oxygen (Park et al., 2002). More variability is observed among the pK_{a2} values due to the presence of the electron-donating alkyl groups attached to the piperazinyl nitrogen in OFL and ENR. Nevertheless, for all three compounds, both pK_a values are such that they are within the range of pH values found in natural waters. Thus, each of the three species (FH_2^+,

FH, and F^-) could be present as a significant fraction in a given water sample and is environmentally relevant.

3.3. Quantum yield determination

It has been observed in previous work that FQ photolysis rates in natural waters exhibit strong pH dependence due to changes in speciation (Ge et al., 2010; Sturini et al., 2010). Here, direct photolysis rate constants (k_{direct}) also varied significantly when experiments were conducted at a pH range inclusive of the pK_a values for each compound. Direct photolysis experiments were performed simultaneously at five pH values ($\sim$ pH 4–10), in three independent trials for each FQ. To illustrate this variability, the fifteen measured values of k_{direct} for all three FQs are shown graphically in Fig. S5.

The degradation rate constants obtained from each of the three series of experiments were deconvoluted to yield calculated rate constants ($k_{direct,calc}$) for each species according to Boreen et al. (2004) and corrected for light screening. The average of the calculated rate constants from the three trials for each FQ is included in Table 2. For all three FQs, the calculated direct photolysis rate for the zwitterionic form (FH) is the fastest, followed by the anionic form (F^-) and finally the cationic form (FH_2^+). For example, the zwitterionic form of NOR is has a rate constant three times larger than the anionic form. Degradation of the cationic form is so slow that the calculated k_{direct} value is not significantly different than zero.

Clearly, small changes in natural water pH will result in large differences in degradation rates for these FQs. Direct photolysis rates at neutral or slightly alkaline pHs where the

Table 2 – Average calculated direct photolysis rate constant, spectral overlap integral, and quantum yield for each species of NOR, OFL, and ENR.

Compound	Protonation state	$k_{direct,calc}$ (s^{-1})/10^{-4}	$\Sigma\varepsilon_{296-450 \text{ nm}}L_{296-450 \text{ nm}}$ (W cm^{-3} M^{-1} nm^{-1})	Φ[a]
Norfloxacin	FH_2^+	–	2.69	–
	FH	84 ± 12	3.32	0.043 ± 0.005
	F$^-$	28 ± 1	3.91	0.013 ± 0.001
Ofloxacin	FH_2^+	–	4.31	–
	FH	6.3 ± 0.8	3.31	0.0030 ± 0.0002
	F$^-$	5.1 ± 0.4	3.87	0.0021 ± 0.0003
Enrofloxacin	FH_2^+	2.7 ± 2.4	3.28	0.0015 ± 0.0013
	FH	91 ± 13	3.22	0.051 ± 0.009
	F-	43 ± 8	3.62	0.022 ± 0.005

a Quantum yields and direct photolysis rates are an average of values obtained in three independent trials, each performed simultaneously at five different pH values. One standard deviation is reported.

zwitterionic form is dominant will be over an order of magnitude faster than at values approximately 2–3 pH units lower. To allow for accurate predictions in a range of natural waters, it must be established whether these differences are attributable simply to variations in absorption spectra or in quantum yields for each species. Absorption spectra obtained at the pH values for which k_{direct} were measured were deconvoluted to yield absorption spectra for each species, in a method similar to that used for the rate constants. These data, in conjunction with emission intensities for the lamp/filter in the solar simulator, were used to calculate quantum yields for each species of each FQ for the wavelength range 296–450 nm using Equation (2)

$$\Phi_{drug} = \Phi_{act}\left[\frac{k_{drug}\sum L_\lambda\varepsilon_{\lambda,act}}{k_{act}\sum L_\lambda\varepsilon_{\lambda,drug}}\right] \qquad (2)$$

where Φ denotes quantum yield, k is the experimentally-derived direct photolysis rate constant, L_λ is the light intensity at a specific wavelength, ε_λ is the molar absorptivity of the compound at that wavelength, subscript act is used to denote a p-nitroanisole/pyridine (PNA) actinometer solution photolyzed alongside each FQ, and subscript drug is used to denote the FQ.

Table 2 shows the spectral overlap integral ($\sum\varepsilon_{296-450 \text{ nm}}L_{296-450 \text{ nm}}$) for each FQ species. These were determined from the deconvoluted absorption spectra, which are shown in Fig. S6. Observed differences in the absorption spectra cannot explain the trends in direct photolysis rates described above. For example, whereas the cationic form of NOR will absorb slightly less light than the zwitterionic form, the anionic form absorbs even more light. For OFL, the cationic form absorbs the most light, yet degrades the most slowly. Thus, there must be differences in quantum yields for each species. Indeed, as shown in Table 2, for each FQ the quantum yield of the zwitterionic species is higher than for the anionic species, and the quantum yield of the cationic species is exceedingly small, essentially indistinguishable from zero. The differences in quantum yields for each species are the dominant reason for FQ photolysis rate variations with pH.

The numbers reported here match well with overall FQ quantum yields that have been reported in previous studies. For NOR, one study gave a value of $\Phi = 0.01$ in pure water, where presumably the dominant form was FH_2^+ with a significant amount of FH present (Fasani et al., 1999a). A study that

measured values for NOR at various pH values found $\Phi = 0.012$ at pH 4.5, $\Phi = 0.06$ at pH 7.2, and $\Phi = 0.005$ at pH 10 (Fasani et al., 1999b). These values are confounded by the fact that the range of pHs tested is broader than that found in natural waters, and additional FQ species beyond the three studied here are present. The general trend, however, matches what is seen here: quantum yields are highest when significant FH is present. For OFL in pure water, $\Phi = 0.0016$ is reported (Fasani et al., 1999a) and for levofloxacin, which is simply the more biologically active enantiomer of the OFL racemic mixture, $\Phi = 0.00826$ in pure water (Ge et al., 2010). Two literature values can be found for ENR in pure water: $\Phi = 0.0697$ (Ge et al., 2010) and $\Phi = 0.00309$ (Burhenne et al., 1997). Again, because there should be some mixture of FH and FH_2^+, these values are reasonable given the quantum yields reported here. To our knowledge, this is the first study to determine quantum yields for each environmentally relevant protonation state of these FQs.

The quantum yield values can be used, in conjunction with the pK_a values, to determine the relative amounts of each FQ species present at a given pH and therefore predict relative direct photolysis rates in whatever natural water system may be of interest. Fig. 2 illustrates the significant variability in calculated direct photolysis rate constants and half-lives that are observed under a range of environmental conditions. The top panels show variation with pH for a specific location and date (St. Paul, Minnesota, solar noon, June 21). Half-lives change dramatically with pH for all three FQs; for example NOR has a half-life of under 2 min at pH 7.7 but this increases to approximately half an hour at pH 5. The bottom panels illustrate, for the pH corresponding to the maximum k_{direct} value of each FQ, how rates vary with latitude and season. Again, tremendous variability is observed; for example, half-lives of ENR at pH 7.2 at mid-latitudes (again at solar noon) range from a couple of minutes during the summer to almost an hour during the winter.

3.4. Photoproduct activity

The work described thus far makes it clear that loss of parent FQ is expected to occur on the order of minutes to hours in sunlit surface waters. These direct photolysis rates, however, refer to loss of parent FQ, not complete mineralization. It cannot be assumed that photolysis of the parent FQ leads to
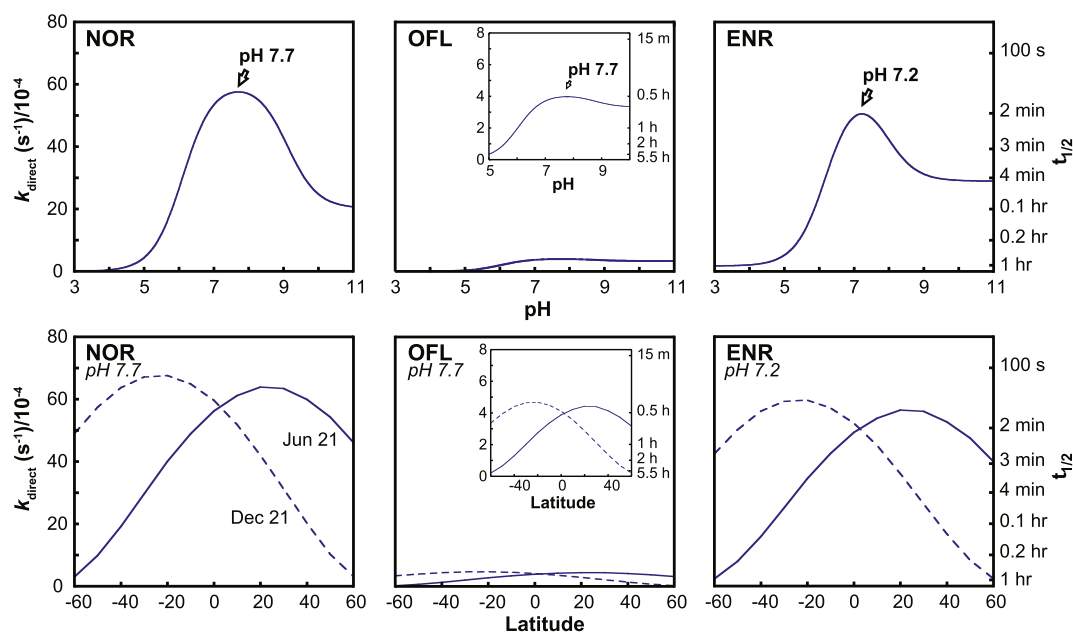
Fig. 2 – Calculated direct photolysis rate constants (k_{direct}, left axis) and half-lives ($t_{1/2}$, right axis) at sea level, solar noon, for NOR, OFL, and ENR. Top panels are calculated for St. Paul, Minnesota (45° north latitude) on June 21 at various pH values. Bottom panels show variation with latitude (all calculated at 0° longitude) for two different seasons (June 21 and December 21) at the pH corresponding to the maximum k_{direct} value for each FQ.

immediate loss of biological activity without knowing the nature of the photoproducts formed. There are many published studies in which FQ photoproducts have been identified, including for the three FQs of interest here (Fasani et al., 1999a; Lam and Mabury, 2005; Ge et al., 2010; Sturini et al., 2010; Li et al., 2011). These reveal much variation, and a complex picture emerges as to the types of products that may occur. The three major types of photolysis reactions that have been reported for FQs under various conditions (some environmentally relevant, some not) include defluorination, decarboxylation, and modifications of the piperazine side chain (Albini and Monti, 2003). The strategy used here was to screen FQ direct photolysis product mixtures for antibacterial activity to allow a rapid assessment of whether products of concern would be likely to form as a result of direct photolysis in natural waters. Paul et al. (2010) previously established lack of residual antibacterial activity for photolysis products of ciprofloxacin (CIP) using a similar strategy. Kusari et al. (2009), however, found that photoproducts of difloxacin (DIF) and sarafloxacin (SARA) retain some potency. Sturini et al. (2012) found mixed results when screening photolysis mixtures of six FQs, including ENR. Minimum inhibitory concentration (MIC) values of a solution including photoproducts were in some cases lower than those of a comparable dilution of parent unphotolyzed FQ, showing transformation products must be retaining some activity.

The overall ability of each irradiated FQ solution to inhibit bacterial growth was used to assess antibacterial activity of the photoproducts. Growth of E. coli DH5α in the presence of each unirradiated FQ, measured as change in optical density, was compared to growth in the presence of a mixture of residual FQ (as measured by HPLC) plus photoproducts

generated at various time points. Fig. 3 shows the results of this antibacterial activity assay. The data were fit with a sigmoidal (Boltzmann) curve fit:

$$y = A_2 + \frac{(A_1 - A_2)}{1 + e^{\frac{x - x_0}{dx}}} \tag{3}$$

where x is log of FQ concentration, y is the change in OD_{600} (ΔOD_{600}), A_1 is the value of y corresponding to no growth inhibition, A_2 is the value of y corresponding to maximum growth inhibition, dx is the slope at the midpoint of the curve, and x_0 is the midpoint. For the irradiated FQ data, the value of A_1 was held to the same value as the corresponding unirradiated FQ data. For the unirradiated fluoroquinolone, the value x_0 corresponds to the concentration of antibacterial compound that is at half its maximum effective concentration (EC_{50}). Because photoproduct concentrations are unknown, this value cannot be correctly called an EC_{50} for the irradiated fluoroquinolone data yet it is a useful value for comparison of antibacterial activity and is used as such here.

The EC_{50} of the unirradiated NOR (0.45 ± 0.02 μM) is similar to the midpoint of NOR plus its photoproducts (0.42 ± 0.01 μM). The same is true for OFL; the EC_{50} for unirradiated OFL is 0.325 ± 0.009 μM, whereas the midpoint for OFL plus its photoproducts is 0.318 ± 0.006 μM. This means that, for these two drugs, all growth inhibition in the irradiated samples can be attributed to residual parent FQ. Additional activity attributable to any photoproducts would result in a decrease of the midpoint value for the irradiated FQ data. Either no products with measurable antibacterial activity are formed during the course of photolysis for NOR or OFL or, if active products are formed, they are not formed at a high enough concentration to have a measurable effect. A previous study which used
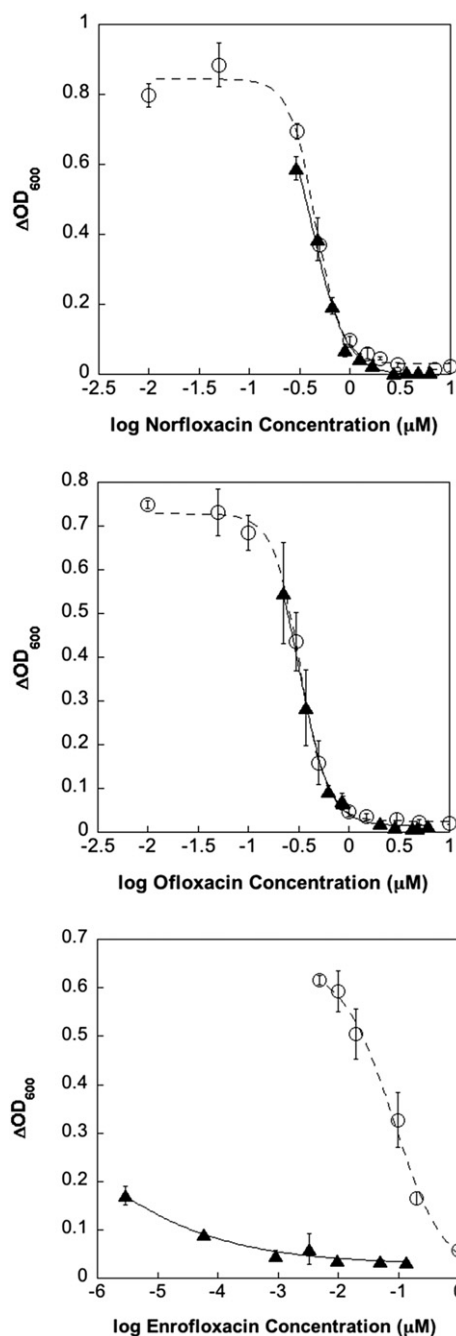
Fig. 3 — Change in optical density at 600 nm (ΔOD_{600}) for *E. coli* DH5α in the presence of a dilution series of unphotolyzed FQ (open circles, dashed line) and residual photolyzed FQ plus photolysis products (closed triangles, solid line) for NOR, OFL, and ENR. Error bars represent one standard error.

a parallel-line bioassay and measured zone of bacterial growth inhibition did see some evidence of active OFL photoproducts (Sunderland et al., 2001), but we did not observe the same effect with our assay.

For ENR, a very different result is observed. The midpoint for ENR plus its photoproducts ($7 \times 10^{-8} \pm 6 \times 10^{-8}$ μM) is substantially lower than the EC$_{50}$ of unphotolyzed ENR

(0.08 ± 0.03 μM). This difference is clear in Fig. 3. At very low residual ENR concentrations, significant growth inhibition is still observed. One or more ENR photoproducts must retain antibacterial activity. This corroborates results of Sturini et al. (2012) who observed a four-fold decrease in MIC for two *E. coli* strains in the presence of ENR photoproducts in comparison to a comparable dilution of unphotolyzed ENR.

3.5. Selected ENR Photoproduct characterization

Photolysis of ENR produced a variety of photoproducts. All products detected were also photolabile so preparative LC was required to achieve isolation of selected products from mixtures of products and any residual ENR. Fig. 4 is a chromatogram generated after approximately one ENR half-life in which four photoproducts present at that point in the photolysis (Products A–D) are highlighted. Products A, B, and D were chosen for isolation and further characterization due to the fact that they had large peak areas within the range of residual ENR concentrations where enhanced antibacterial activity was observed. Product C was only a minor photoproduct but was chosen because chromatographic retention time suggested it was likely CIP, which would be expected to be responsible for a portion of the observed activity. Each of these products was isolated by preparative HPLC, and an accurate mass measurement was then obtained for each product using high-resolution mass spectrometry.

Proposed formulas and structures of each isolated photoproduct are included in Table 3. The accurate mass measurement of Product A matches only one plausible formula if a 5 ppm or less error tolerance is accepted, which yields the proposed structure resulting from the photosubstitution of the fluorine substituent at position 6 by a hydroxyl group. Product B also matches only one plausible formula, and the proposed structure results from both defluorination and degradation of the piperazine side chain. There is variability in the products reported in previous ENR photolysis studies, but both Products A and B were previously observed by Sturini et al. (2010) who characterized Product B on the basis of nominal mass and Product A by nominal mass in conjunction with ^{1}H and ^{13}C NMR. The equivalent
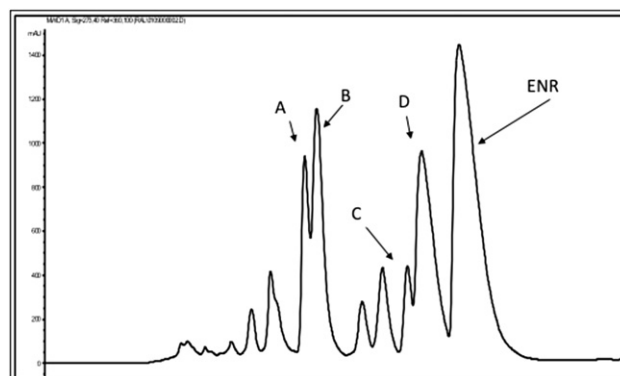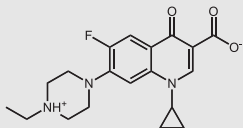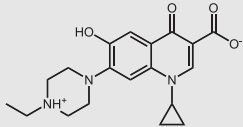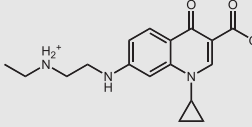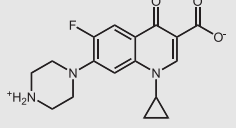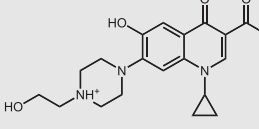

Fig. 4 — Chromatogram produced after ~50% degradation of 500 μM ENR with detection wavelength of 271 nm. Photoproducts that were isolated by prep-LC for further study are labeled A, B, C, and D.

Table 3 – Mass to charge ratio (Da), proposed formula, and proposed structure for ENR and four major ENR photoproducts.

Compound	Measured [M + H]$^+$	Theoretical [M + H]$^+$	Error (ppm)	Proposed formula	Proposed structure
ENR	–	360.1723	–	$C_{19}H_{22}FN_3O_3$	
Product A	358.1769	358.1766	0.8	$C_{19}H_{23}N_3O_4$	
Product B	316.1660	316.1661	0.3	$C_{17}H_{21}N_3O_3$	
Product C (CIP)	332.1415	332.1410	1.3	$C_{17}H_{18}FN_3O_3$	
Product D	374.1713	374.1715	0.7	$C_{19}H_{23}N_3O_5$	

photofragmentation and substitution to Product A has been observed for other FQs including NOR (Fasani et al., 1999a, 1999b). A molecule with the same piperazine degradation as Product B yet maintaining the fluorine at position 6 has been previously observed for ENR (Schmitt-Kopplin et al., 1999; Burhenne et al., 1997).

The most commonly reported ENR photoproduct in previous studies is CIP (Burhenne et al., 1997; Schmitt-Kopplin et al., 1999; Knapp et al., 2005; Ge et al., 2010; Sturini et al., 2010; Li et al., 2011), which was tentatively identified as Product C by chromatographic retention time overlap with an authentic standard. The accurate mass measurement verified this assignment; the formula for CIP was the only plausible formula within 5 ppm tolerable error. Because CIP was the only photoproduct for which an authentic standard was available, it was the only photoproduct for which concentrations could be quantified. In a previous study, CIP was never present as more than 20% of the parent ENR concentration, and not more than 8% under full sun as CIP is also photolabile (Knapp et al., 2005). The same observation was made here. CIP was never observed to be present as more than a small fraction of the parent ENR concentration (no more than 5%, or a maximum concentration of 5 μM for a 100 μM ENR solution).

Unlike for Products A–C, previous work did not help with identification of a structure for Product D. The high-resolution mass spectrum showed that the only plausible formula for the compound is $C_{19}H_{23}N_3O_5$. Sturini et al. (2010) and Li et al. (2011) observed a product with the same nominal mass and both suggested a product with a formula of $C_{19}H_{20}FN_3O_4$. In our study, this proposed product was ruled out since the error is well outside the tolerable accurate mass measurement limits (52.6 ppm). In addition, while we were unable to isolate enough Product D to obtain a clean ^{1}H NMR spectrum of the compound not obscured by mobile phase components, a ^{19}F spectrum of the isolated product showed no fluorine signal. This indicates loss of the fluoro substituent and suggests that photosubstitution of the −OH for the −F substituent at position 6 has occurred. The position of the other −OH substituent is admittedly not as well supported, but we hypothesize the given structure based on similar piperazinyl side-chain modifications observed in previous studies (Burhenne et al., 1997; Sturini et al., 2010).

3.6. ENR photoproduct activity assessment

CIP accounts for some of the enhanced antibacterial activity in the presence of ENR's photoproducts. Given the measured CIP concentrations, however, and the fact that CIP and ENR exhibit almost identical EC$_{50}$ values using the DH5α antibacterial activity assay, the presence of the CIP cannot explain all of the observed activity. This means one or more of products A, B, and D likely retain some activity. All three products retain

the carboxylic acid group at position 3 and the 4-carbonyl moiety, both of which are required for activity. FQs work by inhibiting activity of bacterial type II DNA topoisomerases and the 3- and 4-position substituents are involved in binding to the topoisomerase complex (Domagala and Hagen, 2003). Interestingly, however, none of the three products retain the fluorine in the 6-position. While the presence of the fluorine distinguishes FQs from earlier generation quinolones that, in general, had less activity than the currently used FQ molecules, QSAR studies in recent years have shown that removal of the fluorine in the 6-position does not necessarily dramatically reduce potency (Domagala and Hagen, 2003). Therefore, any of the products could in theory retain activity. Using preparative HPLC, as much of each product as possible was isolated in the same manner as that used to obtain the high resolution mass spectra, and then tested for antibacterial activity. Without an authentic standard it was not possible to measure the concentration of each product, and we were therefore not able to measure EC_{50} values and produce a quantitative comparison of activity such as that for the parent FQs in Fig. 3. It was, however, possible to qualitatively characterize products as active or inactive. No evidence of activity was observed in the presence of a mixture of Products A and B. In the presence of a dilution series of isolated Product D, however, some growth inhibition was clearly observed. Therefore it is highly likely that Product D contributes to at least some of the enhanced activity observed in the presence of ENR photoproducts.

Because all isolated photoproducts, including Product D, are photolabile, it is possible the enhanced antibacterial activity observed for ENR may not have major long-term effects. The fact that activity persists for at least some period of time beyond when ENR itself is present at a significant concentration may be important in certain circumstances. While this work focused only on FQs in an aqueous phase, only a small fraction of FQs that pass through WWTPs are actually present in the effluent. A large portion is retained on the sludge (Giger et al., 2003; Lindberg et al., 2006). In systems where sludge desorption potentially provides a slow, constant route for ENR to enter the environment, the presence of active products may be of note. In addition, ENR is unique in that is it the only antibiotic for which agricultural applications have been restricted due to human health concerns. In 2005, the United States Food and Drug Administration banned the use of ENR in poultry based on its link to emergence of resistant *Camphylobacter* bacteria in chickens and turkeys (FDA, 2005). The knowledge that photoproducts produced in the environment retain activity may add to the concern with the use of this drug in agricultural settings. In general, the result serves as a cautionary note: just because parent FQ concentration has diminished, total activity may not be completely lost. This finding shows the value of screening for product activity when biologically active molecules are transformed in the environment.

4. Conclusions

- Two relevant pK_a values (within the range of pH values expected in natural waters) were determined for the three FQs studied (NOR, OFL, and ENR). This means that each FQ may

exist as one of three major species in natural waters: a cationic form will dominate at values lower than ~pH 6, an anionic form will dominate at values higher than ~pH 8—9, with a zwitterionic form dominant at intermediate pH values.
- Photolysis rate under simulated sunlight was observed to vary significantly with pH for all three FQs and the highest rates were observed at neutral or slightly alkaline pH. This variation in photolysis rate is attributable to significant differences in quantum yields of the three relevant species; the quantum yield for the zwitterionic form is 2—3 times higher than that for the anionic form, and over an order of magnitude higher than that for the cationic form.
- By using a bacterial assay as a screening tool it was determined that NOR and OFL photoproducts do not retain any significant antibacterial activity. ENR photoproducts, however, do retain activity. Only part of this activity is attributable to CIP, which is a minor ENR photoproduct. At least one additional ENR photoproduct retains significant activity.

Appendix A. Supplementary data

Supplementary data related to this article can be found at http://dx.doi.org/10.1016/j.watres.2012.10.025.

REFERENCES

Albini, A., Monti, S., 2003. Photophysics and photochemistry of fluoroquinolones. Chemical Society Reviews 32, 238—250.
Andreozzi, R., Raffaele, M., Nicklas, P., 2003. Pharmaceuticals in STP effluents and their solar photodegradation in aquatic environment. Chemosphere 50, 1319—1330.
Aristilde, L., Melis, A., Sposito, G., 2010. Inhibition of photosynthesis by a fluoroquinolone antibiotic. Environmental Science and Technology 44, 1444—1450.
Boreen, A.L., Arnold, W.A., McNeill, K., 2004. Photochemical fate of sulfa drugs in the aquatic environment: sulfa drugs containing five-membered heterocyclic groups. Environmental Science and Technology 38, 3933—3940.
Burhenne, J., Ludwig, M., Nikoloudis, P., Spiteller, M., 1997. Photolytic degradation of fluoroquinolone carboxylic acids in aqueous solution. Part I: primary photoproducts and half-lives. Environmental Science and Pollution Research 4, 10—15.
Cardoza, L.A., Knapp, C.W., Larive, C.K., Belden, J.B., Lydy, M., Graham, D.W., 2005. Factors affecting the fate of ciprofloxacin in aquatic field systems. Water, Air, and Soil Pollution 161, 383—398.
Domagala, J.M., Hagen, S.E., 2003. Structure-activity relationships of the quinolone antibacterials in the new millennium: some things change and some do not. In: Hooper, D.C.,

Rubinstein, E. (Eds.), Quinolone Antimicrobial Agents, third ed. ASM Press, pp. 3–18.

Fasani, E., Barberis Negra, F.F., Mella, M., Monti, S., Albini, A., 1999a. Photoinduced C-F bond cleavage in some fluorinated 7-amino-4-quinolone-3-carboxylic acids. Journal of Organic Chemistry 64, 5388–5395.

Fasani, E., Rampi, M., Albini, A., 1999b. Photochemistry of some fluoroquinolones: effect of pH and chloride ion. Journal of the Chemical Society, Perkin Transactions 2, 1901–1907.

FDA, 2005. Proposal to Withdraw Approval of the New Animal Drug Application for Enrofloxacin for Poultry. Docket No. 2000N-1571.

Ge, L., Chen, J., Wei, X., Zhang, S., Qiao, X., Cai, X., Xie, Q., 2010. Aquatic photochemistry of fluoroquinolone antibiotics: kinetics, pathways, and multivariate effects of main water constituents. Environmental Science and Technology 44, 2400–2405.

Giger, W., Alder, A.C., Golet, E.M., Kohler, H.-P.E., McArdell, C.S., Molnar, E., Siegrist, H., Suter, M.J.-F., 2003. Occurrence and fate of antibiotics as trace contaminants in wastewaters, sewage sludges, and surface waters. Chimia 57, 485–491.

Golet, E.M., Xifra, I., Siegrist, H., Alder, A.C., Giger, W., 2003. Environmental exposure assessment of fluoroquinolone antibacterial agents from sewage to soil. Environmental Science and Technology 37, 3243–3249.

Hartmann, A., Golet, E.M., Gartiser, S., Alder, A.C., Koller, T., Widmer, R.M., 1999. Primary DNA damage but not mutagenicity correlates with ciprofloxacin concentrations in German hospital wastewaters. Archives of Environmental Contamination and Toxicology 36, 115–119.

Jiménez-Lozano, E., Marqués, I., Barrón, D., Beltrán, J.L., Barbosa, J., 2002. Determination of pK$_a$ values of quinolones from mobility and spectroscopic data obtained by capillary electrophoresis and a diode array detector. Analytica Chimica Acta 464, 37–45.

Knapp, C.W., Cardoza, L.A., Hawes, J.N., Wellington, E.M.H., Larive, C.K., Graham, D.W., 2005. Fate and effects of enrofloxacin in aquatic systems under different light conditions. Environmental Science and Technology 39, 9140–9146.

Kolpin, D.W., Furlong, E.T., Meyer, M.T., Thurman, E.M., Zaugg, S.D., Barber, L.B., Buxton, H.T., 2002. Pharmaceuticals, hormones, and other organic wastewater contaminants in US streams, 1999–2000: a national reconnaissance. Environmental Science and Technology 36, 1202–1211.

Kümmerer, K., 2009. Antibiotics in the aquatic environment – a review – part II. Chemosphere 75, 435–441.

Kusari, S., Prabhakaran, D., Lamshöft, M., Spiteller, M., 2009. In vitro residual anti-bacterial activity of difloxacin, sarafloxacin, and their photoproducts after photolysis in water. Environmental Pollution 157, 2722–2730.

Lam, M.W., Mabury, S.A., 2005. Photodegradation of the pharmaceuticals atorvastatin, carbamazepine, levofloxacin, and sulfamethoxazole in natural waters. Aquatic Sciences 67, 177–188.

Leifer, A., 1988. The Kinetics of Environmental Aquatic Photochemistry, Theory and Practice. American Chemical Society, Washington, D.C., USA.

Li, Y., Niu, J., Wang, W., 2011. Photolysis of enrofloxacin in aqueous systems under simulated sunlight irradiation: kinetics, mechanism and toxicity of photolysis products. Chemosphere 85, 892–897.

Lindberg, R.H., Olofsson, U., Rendahl, P., Johansson, M.I., Tysklind, M., Andersson, B.A.V., 2006. Behavior of fluoroquinolones and trimethoprim during mechanical, chemical, and active sludge treatment of sewage water and digestion of sludge. Environmental Science and Technology 40, 1042–1048.

Lizondo, M., Pons, M., Gallardo, M., Estelrich, J., 1997. Physicochemical properties of enrofloxacin. Journal of Pharmaceutical and Biomedical Analysis 15, 1845–1849.

Park, H.-R., Kim, T.H., Bark, K.-M., 2002. Physicochemical properties of quinolone antibiotics in various environments. European Journal of Medicinal Chemistry 37, 443–460.

Paul, T., Dodd, M.C., Strathmann, T.J., 2010. Photolytic and photocatalytic decomposition of aqueous ciprofloxacin: transformation products and residual antibacterial activity. Water Research 44, 3121–3132.

Prabhakaran, D., Sukul, P., Lamshöt, M., Maheswari, M.A., Zühlke, S., Spiteller, M., 2009. Photolysis of difloxacin and sarafloxacin in aqueous systems. Chemosphere 77, 739–746.

Qiang, Z., Adams, C., 2004. Potentiometric determination of acid dissociation constants (pK$_a$) for human and veterinary antibiotics. Water Research 38, 2874–2890.

Renew, J.E., Huang, C.H., 2004. Simultaneous determination of fluoroquinolone, sulfonamide, and trimethoprim antibiotics in wastewater using tandem solid phase extraction and liquid chromatography-electrospray mass spectrometry. Journal of Chromatography, A 1042, 113–121.

Ross, D.L., Riley, C.M., 1992. Physicochemical properties of the fluoroquinolone antimicrobials. II. Acid ionization constants and their relationship to structure. International Journal of Pharmaceutics 83, 267–272.

Schmitt-Kopplin, P., Burhenne, J., Freitag, D., Spiteller, M., Kettrup, A., 1999. Development of capillary electrophoresis methods for the analysis of fluoroquinolones and application to the study of the influence of humic substances on their photodegradation in aqueous phase. Journal of Chromatography A 837, 253–265.

Sturini, M., Speltini, A., Maraschi, F., Profumo, A., Pretali, L., Fasani, E., Albini, A., 2010. Photochemical degradation of marbofloxacin and enrofloxacin in natural waters. Environmental Science and Technology 44, 4564–4569.

Sturini, M., Speltini, A., Maraschi, F., Pretali, L., Profumo, A., Fasani, E., Albini, A., Migliavacca, R., Nucleo, E., 2012. Photodegradation of fluoroquinolones in surface water and antimicrobial activity of the photoproducts. Water Research 46, 5575–5582.

Sunderland, J., Tobin, C.M., Hedges, A.J., MacGowan, A.P., White, L.O., 2001. Antimicrobial activity of fluoroquinolone photodegradation products determined by parallel-line bioassay and high performance liquid chromatography. Journal of Antimicrobial Chemotherapy 47, 271–275.

Vieno, N.M., Härkki, H., Tuhkanen, T., Kronberg, L., 2007. Occurrence of pharmaceuticals in river water and their elimination a pilot-scale drinking water treatment plant. Environmental Science and Technology 41, 5077–5084.

Wammer, K.H., LaPara, T.M., McNeill, K., Arnold, W.A., Swackhamer, D.L., 2006. Changes in antibacterial activity of triclosan and sulfa drugs due to photochemical transformations. Environmental Toxicology and Chemistry 25, 1480–1486.

Watkinson, A.J., Murby, E.J., Kolpin, D.W., Costanzo, S.D., 2009. The occurrence of antibiotics in an urban watershed: from wastewater to drinking water. Science of the Total Environment 407, 2711–2723.

Wenk, J., von Gunten, U., Canonica, S., 2011. Effect of dissolved organic matter on the transformation of contaminants induced by excited triplet states and the hydroxyl radical. Environmental Science and Technology 45, 1334–1340.

Xu, W.H., Zhang, G., Zou, S.C., Ling, Z.H., Wang, G.L., Yan, W., 2009. A preliminary investigation on the occurrence and distribution of antibiotics in the yellow river and its tributaries, China. Water Environment Research 81, 248–254.